MJFAS
Malaysian Journal of Fundamental and Applied Sciences

Mohd Saidi *et al.* | Malaysian Journal of Fundamental and Applied Sciences, Vol. 22 (2026) 583-602

RESEARCH ARTICLE

Effect of Electrodeposition Conditions and Sn:Co Ratio on SnCo-Modified Carbon Electrodes for Cathodic Reactions and Microbial Fuel Cell Performance

Nor Syazwanie Mohd Saidi, Yashawini Phriya Rauichandran, Muhamad Amirul Aiman Mohd Nor, Norhamizah Hazirah Ahmad Junaidi, Irwan Ibrahim, Wai Yin Wong, Swee Su Lim*

Fuel Cell Institute (SELFUEL), Universiti Kebangsaan Malaysia, 43600 UKM Bangi, Selangor, Malaysia.

Abstract The performance of microbial fuel cells (MFCs) is commonly limited by the sluggish oxygen reduction reaction (O_2RR) at the cathode, which reduces electron acceptance and overall power generation. Therefore, the development of low-cost and stable cathode catalysts is important to improve MFC performance. In this study, SnCo-based electrocatalysts were developed as alternative cathode materials to enhance cathodic reduction reactions in bioelectrochemical systems. Tin (Sn) was introduced into cobalt (Co)-based catalysts to improve catalytic behaviour, active-site availability and structural stability. The study was conducted in two screening parts. First, SnCo was electrodeposited onto carbon felt at different deposition potentials from −0.2 to −1.2 V to evaluate carbon dioxide reduction reaction (CO_2RR) activity and surface morphology. Carbon felt deposited at −0.6 V showed the highest CO_2RR current density, although surface analysis showed that the deposits did not fully cover the carbon felt. Secondly, SnCo was deposited onto carbon cloth at Sn:Co ratios of 1:1, 1:2 and 1:4 to evaluate O_2RR activity, stability and MFC cathode performance. Response surface methodology (RSM) identified −0.6 V and SnCo 1:4 as the most favourable electrochemical screening condition based on the selected CO_2RR and O_2RR responses. However, MFC validation showed that SnCo 1:2 achieved the highest maximum power density of 0.105 W m^{-2}, followed by SnCo 1:1 at 0.089 W m^{-2} and SnCo 1:4 at 0.069 W m^{-2}. This indicates that electrochemical screening does not directly translate to whole-cell MFC performance. Overall, SnCo-modified carbon electrodes show potential as low-cost cathode catalysts for bioelectrochemical systems.

Keywords: SnCo electrocatalyst, microbial fuel cell (MFC), oxygen reduction reaction, carbon dioxide reduction reaction, energy recovery.

***For correspondence:**
limss@ukm.edu.my

Received: 27 January 2026
Accepted: 25 May 2026

Introduction

The increasing concentration of atmospheric CO_2 represents one of the most challenging environmental problems throughout the years. As the primary greenhouse gas driving global climate change, CO_2 accumulation has led to rising global temperatures, ocean acidification, and widespread ecological imbalance [1], [2] According to Global Energy Review 2024 reported by the International Energy Agency, the global CO_2 emissions has increased by 0.8% compared to the year 2023, reaching an all-time high number of 37.8 Gt of CO_2 and an atmospheric concentration of 422.5 ppm [3]. Human activities such as industrial operations like fossil fuel industry, ground transportation, aviation, fishing, international shipping activities as well as commercial and residential building industries have contributed to CO_2 emissions [4]. Specifically, fossil fuel is the main source of conventional power generation systems, which are widely utilised especially by developing countries with an average of more than 79% of their electricity relying on it [5]. In addition to these activities, biological processes such as wastewater treatment plants also contribute to global CO_2 emissions, as these plants produce CO_2, nitrous oxide (N_2O) and methane (CH_4) [6], although it is necessary. To address this problem, a system that combines pollution control and reduces CO_2 [6], [7], [8] is needed. One approach is through the utilisation of wastewater in microbial

fuel cells. Wastewater can be used as renewable chemical energy source in this system. This provides better electricity generation while simultaneously reduces carbon footprint of wastewater treatment [9].

Microbial Fuel Cell (MFC) is considered as a suitable alternative for waste management and energy generation. The principle of MFC involves microorganisms that are electrochemically active. These microorganisms feed on the organic matter in the wastewater and respire extracellularly by transferring electrons to the anode. In the presence of oxygen, the electrons flow through the external circuit from the anode to cathode for reduction reaction to occur. This will produce electrical energy while the wastewater is treated [10], [11]. One of the advantages of MFC is it can utilise diverse biomass as a substrate with minimal energy input. In addition, MFC allows direct energy conversion via bio-electrocatalytic processes and can operate under ambient conditions. Moreover, the system's capability to simultaneously treat wastewater and generate electricity with low-cost materials and environmentally friendly approach demonstrates the practicality and sustainability of the system [9].

The performance and efficiency of MFC are influenced by various factors such as electrode materials, pH of wastewater, microbial inoculum, reaction kinetics and reactor configuration [12] The development of new electrode materials can improve the functions and the output of the MFC system. Previously, various carbon-based materials such as carbon cloth, carbon mesh and graphite fibers have been widely explored as electrodes [13]. However, they have relatively low electrochemical performance which limits their overall performance in MFC. This limitation has reduced the efficiency of MFC system and decreased the practicality of the technology, creating a challenge in the application. The challenge lies in the sluggish oxygen reduction occurring at the cathode [12]. O_2 serves as the terminal electron acceptor in MFC, which is crucial for power generation within the system. This slow O_2RR kinetics is caused by the neutral media in which MFC is operating, leading to low concentrations of H^+ and OH^-. The low concentrations of both ions reduce the overpotentials and the kinetics. Slow O_2RR kinetics decrease the overall performance [11]. Metal catalysts have been developed to overcome this challenge. The right catalyst will improve the power output. Enhanced power output will increase the efficiency of MFC system [14].

The most commonly used catalyst is Pt. This is due to the high electrical conductivity, high chemical stability and high resistance to corrosion possessed by the metal, which makes it suitable for long term operation. Despite these advantages, the sources of Pt are limited and expensive. Due to these shortcomings, the studies on developing alternative catalysts for cathode electrodes have been increasing [15]. These studies focus on producing highly available economical electrodes with excellent conductivity. For example, tungsten oxide/polyprrole (WO_3/Ppy) has been studied by [16].In the study, it was found that the power density produced was 0.571 Wm^{-2} which was comparable to Pt with power density 0.84 Wm^{-2}. Other than that, a study on Cu-metal organic framework@Fe-metal (Cu-MOF@Fe-MOF) has found it to produce maximum power density of 231.2 mV/m^2 [17]. These studies have proven that other metals have the potential to be as good as Pt as catalysts.

Transition metals such as Co, Mn and Cu have been explored as catalysts for the development of cathode electrodes due to their electrochemical properties [18]. Co, specifically, has properties such as having multiple oxidation states, which facilitate electron transfer and support the formation of Co–O and Co–OH intermediates. This allows for efficient O_2RR. However, the use of Co as catalyst has its own challenges which include easily corroded and limited active sites. This reduces the stability and the efficiency of the electrodes. To overcome this shortcoming, Co is doped or integrated with other elements. Previous research on Co-based catalysts done by [19], [20], [21] and [22] has shown enhancements in oxygen reduction activity in the MFC system. The study by [19] demonstrated Co doped with heteroatoms nitrogen, carbon and sulphur had better stability than undoped Co and maintained high O_2RR activity after 10 000 cycles. The heteroatoms coordinated synergistically with Co, enhancing the durability in harsh electrochemical environments [19]. Besides heteroatoms, one approach is through doping with Sn. Recent findings indicate that Sn-doped Co-based catalysts have shown great improvement in catalytic activity especially in CO_2 reduction [23]. Sn aids in altering the electronic structure, renewing the active sites of the electrodes, changing the mass transfer and improving conductivity of the produced catalyst. The use of Sn is also considered cost-effective [24], [25]. Despite its potential, the study of Sn as an electrochemical catalyst is still limited. This research gap highlights the need to understand the properties and mechanisms of Sn so that its potential can be maximised.

This study focuses on examining SnCo-modified carbon electrodes through two screening parts. First, carbon felt was deposited with SnCo at different deposition potentials to analyse the effect of deposition potential on the electrochemical activity and morphology of the produced electrodes. The CO_2 reduction study was conducted to evaluate the potential of SnCo-deposited carbon felt in promoting cathodic reduction behaviour under neutral aqueous conditions. Carbon felt was selected for this screening part

because it is a commonly used carbon-based electrode material in MFC studies. Its high surface area and porous structure are also beneficial for electrolyte penetration and catalyst deposition [13]. To align with the goal of improving cathodic reactions in MFC-related systems, this CO_2RR study serves as a preliminary assessment to understand how SnCo deposition conditions influence the catalytic behaviour of the material.

Secondly, SnCo was deposited on carbon cloth with different Sn:Co ratios of 1:1, 1:2 and 1:4. The O_2 reduction activity of the deposited carbon cloths was measured to determine their efficiency towards O_2RR, as cathodic oxygen reduction is one of the main factors controlling power generation and overall MFC performance [12],[14]. Carbon cloth was selected for this part due to its sheet-like structure, mechanical stability and suitability for assembly as a cathode in the MFC reactor. This selection is also consistent with the common use of carbon cloth as a carbon-based electrode material in MFC studies [13]. Therefore, the carbon felt and carbon cloth experiments were not intended as a direct substrate-to-substrate comparison, but as two screening parts to evaluate SnCo catalytic behaviour under different cathodic reaction conditions.

As carbon cloth showed good stability during prolonged oxidative activity, the SnCo-deposited carbon cloths with different ratios were further applied in the MFC system to evaluate their practical cathode performance. This O_2RR-focused investigation forms the core objective of the study, as it directly evaluates the suitability of SnCo as cathode catalysts in MFCs. Overall, the CO_2 reduction study on carbon felt provides preliminary information on the potential of SnCo deposition for cathodic reduction applications, while the O_2 reduction and MFC study on carbon cloth directly support the main aim of enhancing O_2RR performance and improving MFC power generation efficiency. This approach allows the electrochemical behaviour of SnCo-modified electrodes and their practical application in MFC cathodes to be evaluated in a more systematic manner.

Materials and Methods

All materials and chemicals used in this study were handled under controlled laboratory conditions to maintain accuracy throughout the experimental processes. The materials used include carbon felt, carbon cloth, tin (II) chloride dihydrate ($SnCl_2{\cdot}2H_2O$), cobalt (II) chloride hexahydrate ($CoCl_2{\cdot}6H_2O$), deionized water (DI), 1 M and 3 M hydrochloric acid (HCl), 0.2 M ethylenediaminetetraacetate (EDTA), 1 M sodium hydroxide (NaOH).

The apparatus used include beaker (100 mL, 500 mL), volumetric flask (100 mL, 250 mL), glass rod, magnetic stirrer, spatula and weighing tray. Potentiostat (Metrohm AUTOLAB PGSTAT128N, Switzerland) was used for deposition.

Preparation of SnCo electrolyte

To prepare the electrolyte for carbon felt deposition, $SnCl_2$ and $CoCl_2$ were prepared with 1:1 ratio using EDTA as chelating agent. Chelating agent was added to stabilise and enhance the electrodeposition method. EDTA alone was used for carbon felt because the study focused on deposition-potential screening at a fixed Sn:Co ratio in acidic condition. Chelating agent will form stable bonds with Sn^{2+} and Co^{2+} ions, aiding uniform deposition onto the carbon substrate. $SnCl_2$ was first added into a pre-heated (~60℃) 3 M HCl in a beaker and stirred until the cloudy solution became clear. After that, $CoCl_2$ was added until fully dissolved. The solution turned bluish-purple. Once dissolved, 0.2 M EDTA was added dropwise to avoid vigorous reaction that would cause small aggregates to form. Finally, the solution turned light purple. The pH of the solution was measured. To dilute the solution to 0.05 M, the solution was added with 250 mL deionized water in a volumetric flask.

To prepare the electrolyte for carbon cloth deposition, $SnCl_2$ and $CoCl_2$ were prepared with the Sn:Co ratio of 1:1, 1:2 and 1:4 as shown in Table 1. The solution was acidified first with H_2SO_4 to prevent the hydrolysis of Sn^{2+} and the formation of any Sn salts that can interfere with the deposition. After the initial acidification, the pH of the solutions was adjusted to 7 using standardised aqueous solutions of NaOH and HCl before the deposition. KNa tartrate was added with EDTA to improve electrolyte stability at pH 7 and support controlled SnCo co-deposition during the Sn:Co ratio screening as Sn is easily hydrolysed in neutral condition.

Table 1. The composition of materials in the electrodeposition of carbon cloth

Composition	Sn:Co ratio		
	1:1	1:2	1:4
$CoCl_2$	0.1 M	0.14 M	0.16 M
$SnCl_2$	0.1 M	0.07 M	0.06 M
EDTA	0.2 M	0.2 M	0.2 M
KNa Tartrate	0.2 M	0.2 M	0.2 M
pH	7	7	7

Fabrication of electrodes

Activation of carbon felt and carbon cloth

Carbon cloth electrodes underwent a sequential cleaning and activation process. This involved ultrasonication in ethanol for 15 minutes to remove contaminants followed by chemical activation through the immersion in 1 M H_2SO_4 and then 1 M NaOH, each for 30 minutes. Once activated, the electrodes were dried at 60℃ and stored in a desiccator until further use.

Electrodeposition of SnCo onto carbon felt and carbon cloth

For carbon felt, the cell was set up with carbon felt as counter electrode and Ag/AgCl as reference electrode. The working electrode, carbon felt was cut with effective area of 2 cm^2 (2 cm × 2 cm). The deposition was done via chronoamperometry. Six potentials, -0.2 V, -0.4 V, -0.6 V, -0.8 V, -1.0 V and -1.2 V versus Ag/AgCl were chosen as the potentials for electrodeposition of SnCo on the carbon felt. After that, the electrodes were thoroughly rinsed with DI water and left to dry at 60℃. For carbon cloth, the electrodeposition was set up with a titanium wire as the counter electrode and an Ag/AgCl reference electrode. The working electrode, carbon cloth was cut with effective area of 25 cm^2 (5 cm × 5 cm). The deposition was done via cyclic voltammetry (CV). CV were performed at a rate of 10mV/s within a potential window of 0 V to 1.5 V versus Ag/AgCl reference electrode. Then, the electrodes were thoroughly rinsed with DI water and left to dry at 60°C.

Electrochemical analysis of SnCo deposited electrodes

Cyclic voltammetry analysis

CV analysis was performed to measure the catalytic activity performance of produced SnCo electrodes. CV analysis of SnCo deposited carbon felt were done in CO_2-saturated 0.5 M phosphate buffer solution (PBS) in saturated CO_2 at pH 7. The analysis was done using the standard three-electrode system. Deposited carbon felt was the working electrode and undeposited carbon felt was used as the counter electrode. Ag/AgCl was the reference electrode. The scan rate for the analysis was 50 mV. The range of potential used was -1.5 V to +0.5 V versus Ag/AgCl.

CV analysis of SnCo deposited carbon cloth were done in N_2 and O_2- saturated 0.1 M KOH. Similar to carbon felt, CV analysis of SnCo deposited carbon cloth were done using the standard three-electrode system. The working electrode was the deposited carbon cloth, and titanium rod was used as counter electrode. Ag/AgCl was the reference electrode. The scan rate used was also 50 mV. The range of potential used was 0 to 1.1 V versus RHE. All scans were performed at room temperature and repeated three times to ensure consistency and reproducibility.

Chronoamperometry (CA) analysis

CA analysis was performed to assess the stability and durability of the electrodes. The current response was recorded over a duration of 10 000 seconds at a fixed potential to observe the long term electrocatalytic performance of each electrode. For SnCo deposited carbon felt, the potential used was -0.6 V versus Ag/AgCl whereas for the carbon cloth, the potential used was 0.6 V versus RHE. The potential chosen was based on the CV analysis. -0.6 V was chosen for carbon felt because it is within the range of CO_2 reduction that occurred for the electrode. 0.6 V was chosen for carbon cloth because it is within the range of O_2 reduction.

Surface analysis

The surface morphology of the electrodeposited carbon electrodes were examined using field emission scanning electron microscopy (FESEM) with a GeminiSEM 500 microscope to study on the morphology, providing details on the shapes and sizes of features on the sample's surface.

Cell setup, operation and monitoring

For this study, the dual-chamber microbial fuel cells (MFCs) were constructed from perspex two pieces

of polyacrylic blocks size (7 cm x 7 cm x 2 cm) with a final operational volume of 50 mL. It consisted of anode and cathode chambers with each of them having 25 mL operating volumes. Both the cathodic and anodic compartments were separated by cation exchange membranes (CEM) (CMI-7000, Membranes International Inc., USA). Plain carbon cloth (Ø 40 mm) was trimmed into a size of 5 cm x 5 cm as an anode. The same size of carbon cloth was used as a cathode with additional SnCo being electrodeposited. Titanium plate (Ti-shop.com, William Gregor Ltd, UK) was used as a connector to link the terminals to a power supply (Quadpotentiostat, Whinstonbrook, UK). Figure 1 shows the schematic of the MFC and lab-scale MFC used.

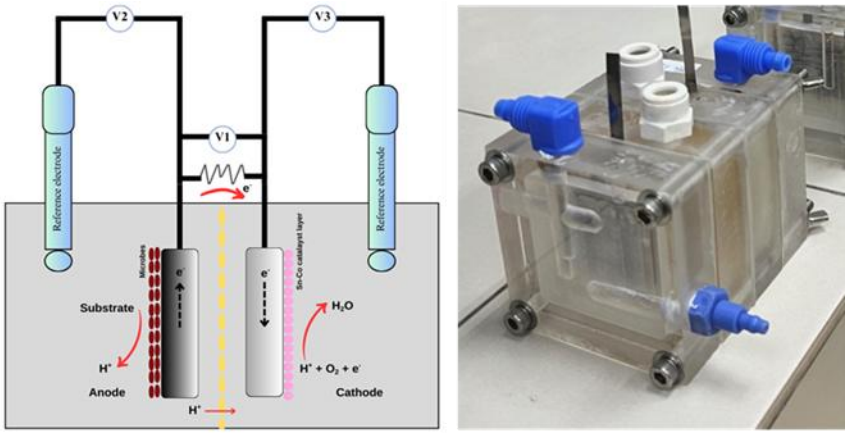

Figure 1. Schematic (on the left) and lab-scale (on the right) microbial fuel cell (MFC)

Inocula were derived from biofilm cultures collected from Tasik Kejuruteraan, Universiti Kebangsaan Malaysia and enriched with enrichment medium. The inocula were premixed with fresh medium (50% v/v) before being injected into the MFC systems. The medium was prepared in accordance with [26] which involves the preparation of phosphate buffer (50 mM) only for the cathode and phosphate buffer (50 mM), ammonium (5 mM), acetate (10 mM), vitamins, and trace minerals for the anode respectively. A fixed voltage of 0.3 V was applied to the MFC cells unless stated otherwise. Ag/AgCl reference electrodes were located at the anode and cathode to provide half-cell potential references. The cell voltage (V1) and anode (V2) and cathode (V3) potentials were monitored using a multichannel data logger (NI-USB-6225, 189 National Instruments, UK).

Experimental design for optimisation of parameters

Response surface methodology (RSM) was employed to evaluate the combined influence of electrodeposition potential and Sn:Co compositional ratio on the electrochemical performance of SnCo catalysts. Rather than using a predefined experimental design, a second-order polynomial model was fitted to an experimentally defined grid of conditions selected based on electrochemical constraints. Deposition potential was varied between -0.20 and -1.20 V, while the Sn:Co ratio ranged from 1:1 to 1:4. The response variable corresponded to the normalised electrochemical performance obtained from cyclic voltammetry measurements.

The experimental data were analysed using a quadratic regression model of the form $Y = \beta_0 + \beta_1 C + \beta_2 V + \beta_{11} C^2 + \beta_{22} V^2 + \beta_{12} CV$, where C represents the Co ratio and V represents the deposition potential. Model coefficients were estimated by least-squares regression, and analysis of variance (ANOVA) was used to assess overall model significance. Model adequacy was further evaluated through residual diagnostics, including normal probability plots and residuals versus fitted values. Statistical analyses were performed using Microsoft Excel (Analysis ToolPak), and three-dimensional response surface plots were generated from the fitted model to visualise parameter interactions and identify optimal conditions.

Results and Discussion

Electrodeposition of SnCo on carbon felt and carbon cloth

Figure 2 shows the chronoamperometric curves of SnCo depositions using -0.2 V, -0.4 V, -0.6 V, -0.8 V, -1.0 V and -1.2 V during the second round of deposition. Overall, the curves only have slight curve at the beginning before becoming flat almost throughout the depositions for all potentials. Carbon felt is a

porous 3D electrodes which the system reaches a quasi-steady-state that is controlled by the transport inside the porous network [27], instead of the planar Cottrell $t^{-1/2}$ decay, causing almost constant current throughout. Other than that, if the flow is restricted in the xy-plane (in-plane) of the electrode, it can cause stagnation of flow [28]. The magnitude of current density increases as more negative potential was applied. Generally, this means more metals have been reduced especially if it is in the limiting potential range. As the potential gets more negative, more charge was being passed and large fraction of these charge might go to the hydrogen evolution. Hence, the deposition is not efficient [29]. Based on the curves, there is only slight increment of current with each increasing potential. This could be due to the limitation of mass transport within the carbon felt or the electron-transfer kinetics is already fast that makes any overpotential less effective [27].

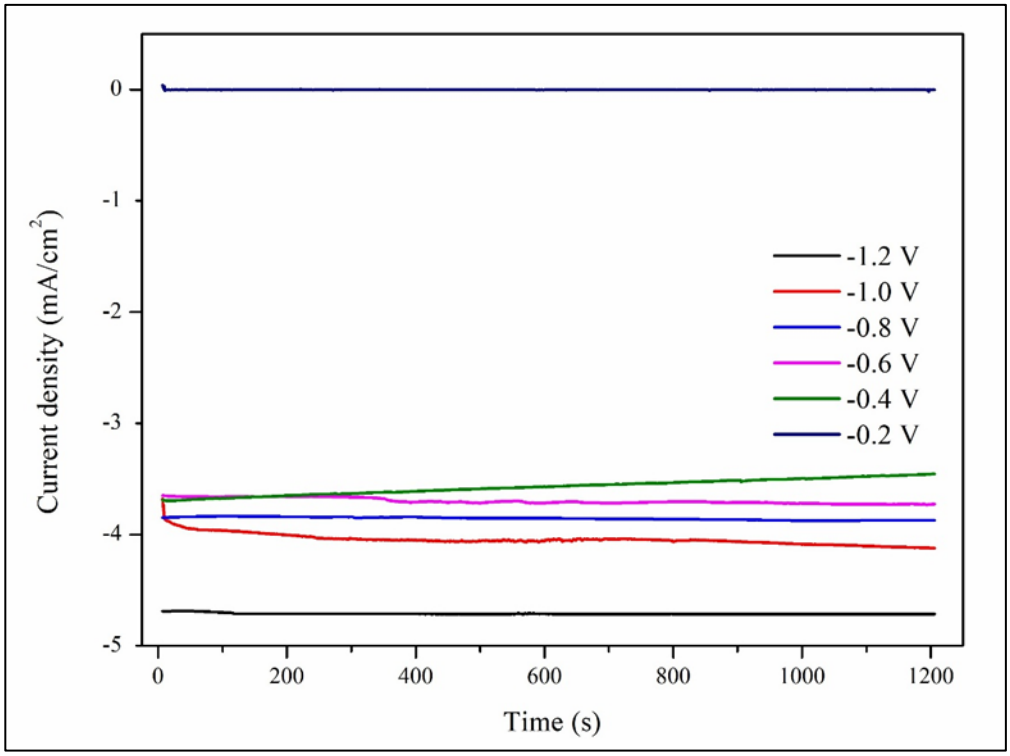

Figure 2. Chronoamperometric curves of SnCo depositions at -0.2 V, -0.4 V, -0.6 V, -0.8 V, -1.0 V and -1.2 V

It is observed that the current for -0.2 V was near zero and remained steady throughout the deposition. This indicates that there was little to no deposition occurring. This is because at this potential, -0.2 V might be too small to reduce Sn^{2+} or Co^{2+} ions to metals as the reduction potential of Sn^{2+} and Co^{2+} against Ag/AgCl are -0.34 V and -0.48 V respectively. The deposition of Sn^{2+} to Sn metal might have started at this potential. However, due to little deposition, the current produced was low. The magnitude of current shows high increment from -0.2 V to -0.4 V, indicating that deposition has probably increased at that potential. As the reduction potential of Sn is more positive than Co, it is expected that Sn started to deposit first. According to [30], the Sn^{2+} will start to deposit at the potential -0.6 V with peak current at -0.8 V.

From the observation, as the potential increases, the current density also increases. At -1.2 V potential, it can be observed that the current density increases steeply compared to -1.0 V. Due to high potential, the deposition competes with the hydrogen evolution reaction (HER) which causes the extra current. At this potential, HER and deposition might occur simultaneously which changed the nucleation and the mechanism of growth for the deposition [31].

It is also suggested that, due to the competing hydrogen evolution, this causes rough deposition with poor adhesion, weakening the deposition which makes it easily fall off of the carbon felt [32]. H_2 bubbles could also be seen during the deposition. The bubbles cannot be removed from the electrolytes quickly. These bubbles will accumulate on the surface of the electrode. This reduces the active area on the surface which will make less efficient deposition [33].

Figure 3 shows the deposited electrodes with different potential. It can be observed that the deposited electrodes using -0.2 V, -0.4 V and -1.2 V of applied potential against Ag/AgCl have no deposition that can be seen with the naked eyes whereas for the deposited electrodes using -0.6 V, -0.8 V and -1.0 V, shiny grey coating can be seen on the surface of the electrodes.

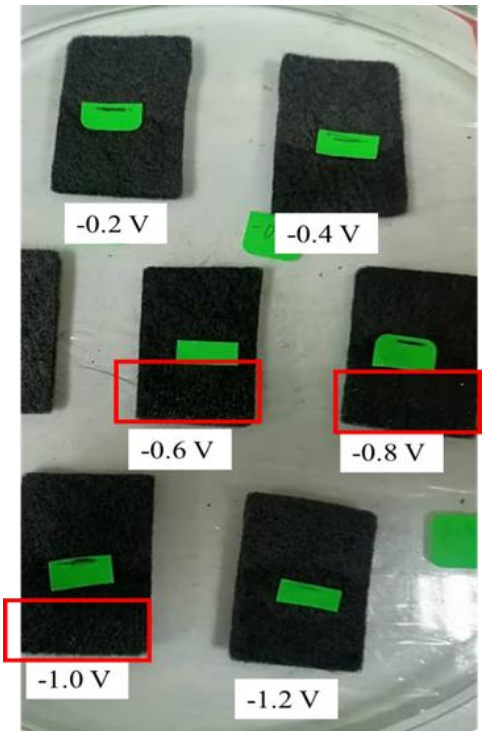

Figure 3. SnCo deposited carbon felts at different potentials

Electrochemical activity of SnCo deposited carbon felt and carbon cloth

Figure 4 shows the cyclic voltammograms of SnCo deposited carbon felts using -0.2 V, -0.4 V, -0.6 V and -0.8 V, -1.0 V and -1.2 V. Based on the figure, the CO_2 reduction peak is at -0.5 V to -1.5 V. It can be observed that the CO_2 reduction occurred from -0.75 V to -1.25 V with the peak at ~-0.85 V.

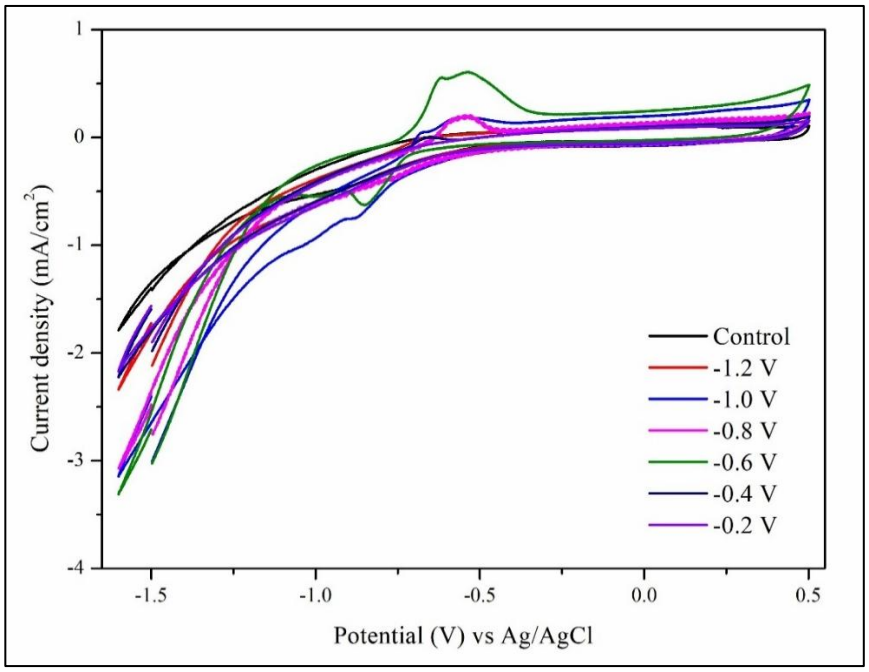

Figure 4. Cyclic voltammograms of SnCo deposited carbon felts at -0.2 V, -0.4 V, -0.6 V, -0.8 V, -1.0 V and -1.2 V

Figure 5 shows the oxidation current of CO_2 reduction activity measured at -0.6 V vs Ag/AgCl varied with the SnCo deposition potential. Electrodes deposited at potentials (-0.6 to -1.0 V) exhibited higher cathodic currents, indicating good SnCo composition and accessible active sites. In particular, the -0.8 V deposited electrodes shows a sharp decrease in CO_2RR current at -0.6 V. This is probably due to the lack of deposition due to poor adherence or non-uniform distribution of SnCo on the carbon felt due to low deposition efficiency. This reduces the CO_2 reducing properties of the felt [34], [35]. Hydrogen evolution that might occur during the deposition has thinned the diffusion layer. The surface morphology changed from compact grains to porous and dendritic structure. This has negatively impacted the properties of the electrode produced due to the hydrogen permeation into the surface [36].

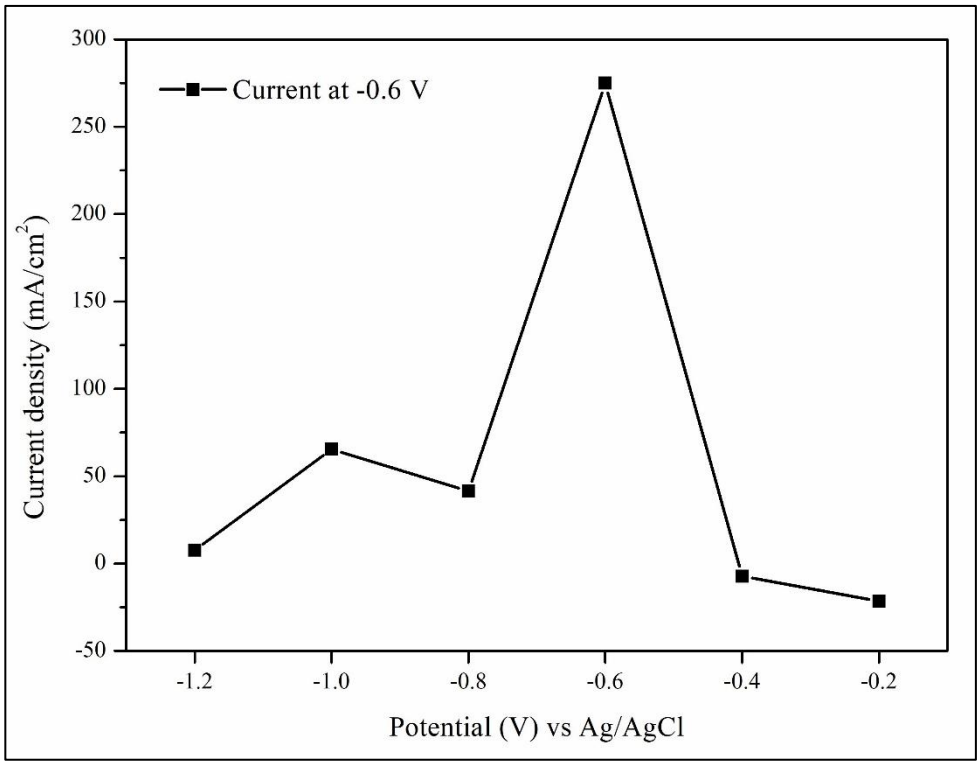

Figure 5. Oxidation current at -0.6 V from cyclic voltammograms

Figure 6 shows the cyclic voltammograms of SnCo deposited carbon cloth using Sn:Co ratios of 1:1, 1:2 and 1:4. The oxygen reduction activities of the SnCo catalysts were measured in both nitrogen- and oxygen-saturated electrolytes, with the potential scanned from 0 to 1.1 V vs RHE. Based on the figure, all SnCo electrodeposited samples showed an increase in the current density under oxygen-saturated conditions compared to nitrogen, confirming their activity toward the O_2RR and proves the success of the electrodeposition onto the carbon cloth. Distinct oxygen reduction peaks can be observed, with O_2RR potential (E_{ORR}) around 0.55 V vs RHE, and an onset potential (E_{onset}) ranging between 0.70–0.75 V vs RHE. This activity is likely due to the presence of metallic (non-oxidised) Sn and Co species uniformly deposited on the carbon cloth surface [37], [38]. Moreover, a more positive shift in both E_{ORR} and E_{onset} can be observed when the cobalt precursor concentration is increased, suggesting that cobalt plays a crucial role in facilitating oxygen reduction reaction.

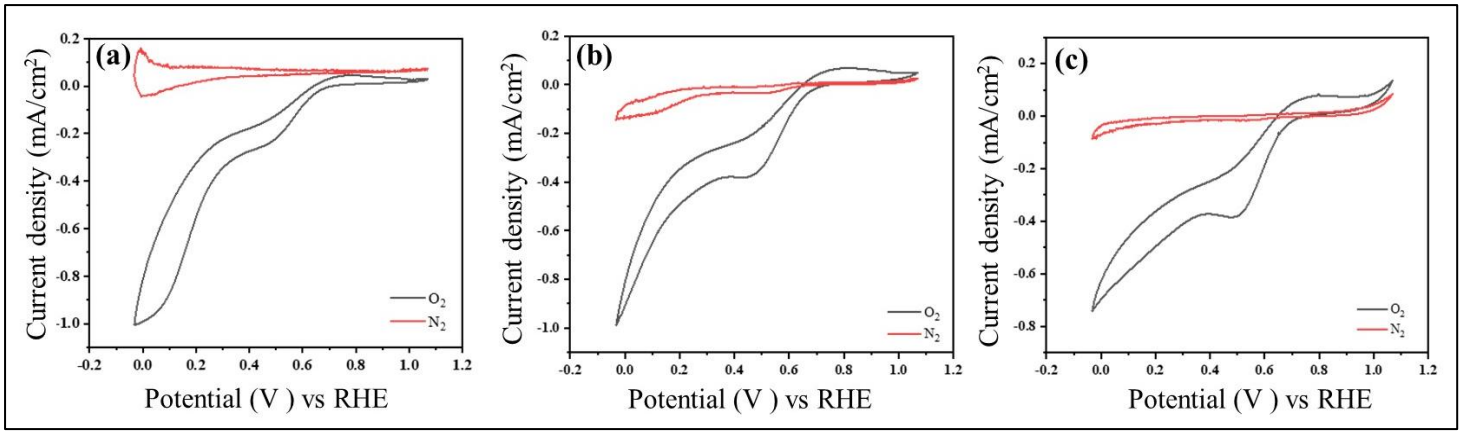

Figure 6. Cyclic voltammetry analysis in saturated-O_2 of SnCo deposited carbon cloths with (a) 1:1 ratio, (b) 1:2 ratio and (c) 1:4 ratio

Stability study of electrodes

Chronoamperometric analysis of SnCo deposited carbon felt and carbon cloth

Current retention based on the chronoamperometric curves of SnCo deposited carbon felts and carbon cloths for 10 000 seconds is shown in Figure 7. For deposited carbon felts, the lowest potential, -0.2 V, -0.6 V and the highest potential -1.2 V were chosen for stability study. From the chronoamperometric curves obtained, -0.2 V showed the highest current retention at 73%, followed by -0.6 V at 44% and -1.2 V has the lowest current retention at ~30% after 10 000s. The variation in stability is caused by the different composition of Sn and Co. At -0.2 V, Sn deposited before Co because the more positive standard reduction potential. The composition of Sn on the surface is higher of Co, making the effect of Sn more prominent. The presence of Sn can improve the structural stability of catalyst [39]. This makes the electrode able to maintain its current for long time.

Despite having the highest current density in CO_2 reduction, carbon felt deposited at -0.6 V, the low percentage of current retention is due to Ostwald ripening, coalesce and leaching of the catalyst into the electrolyte [40]. The lowest current retention shown by carbon felts deposited at -1.2 V is because of the poorly-adhered metal clusters and partial film formation on the surface as shown in SEM image. These structures are prone to cracking or peeling due to mechanical fragility. During the deposition, the composition of SnCo ratios also changed with increasing potential. The deposition at extreme overpotential can cause electrochemical instability as the surface can have poor electronic contact and localized corrosion during prolonged operation.

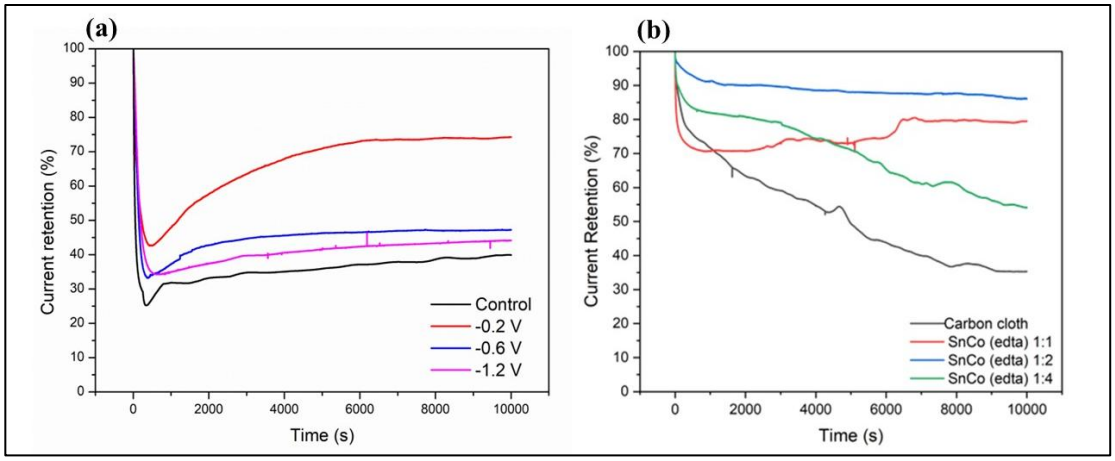

Figure 7. Current retention of (a) carbon felts and carbon cloths after 10 000 s activity

The SnCo 1:2 sample exhibited highest current retention, maintaining over 85% of its initial current, followed by the SnCo 1:1 sample, which sustained about 80%. These results highlight the essential role of Sn in improving the chemical stability of the catalyst layer. Despite having high O_2RR activity, SnCo 1:4 sample experienced current degradation, representing the similar trend as bare carbon cloth (CC). This can be attributed to the reduced Sn:Co ratio in the precursor solution, the very thin layer of catalyst deposited on the CC and limited active site availability. These results indicate that a balanced metal composition not only improves activity but also enhances long-term operational stability. This finding aligns with previous literature, which emphasizes that optimal metal ratios and structural integrity are essential for sustaining catalytic performance in energy conversion devices [41].

Surface analysis of electrodes

Figure 8 and Figure 9 show the SEM micrographs of SnCo deposited carbon felts using 1000× magnification and 3000× respectively. Overall, it can be seen that the deposits did not fully cover the carbon felts. The deposited SnCo were embedded to the fibers in the carbon felt. For carbon felt deposited at -0.2 V, smooth carbon felt surface can be observed in Figure 8(a). It can be seen from the figure; deposition has occurred at this potential. However, there are only a small number of extremely fine particles observed on the carbon fibers. This indicates that although the deposition has occurred, the applied potential was only sufficient for the growth of very small particles. As the potential increased

to -0.4 V, well-defined nuclei began to form as seen in Figure 8 & 9(b). The overall coverage was sparse and isolated.

The size distribution became more uniform at -0.6 V. There were more deposits compared to -0.4 V. Based on electrochemical reduction of CO_2, the reduction shown by -0.6 V was better than -0.4 V and -0.2 V. This could be attributed to the amount of the deposits and the particle size distribution. More deposits increased the active sites for the CO_2 reduction activity to occur [42]. The deposits were distributed more evenly along the fibers surface. This suggests enhanced nucleation. There were more metals being deposited onto the surface of carbon fibers the potential of -0.8 V. The aggregates of deposits on carbon felt were more even too. From Figure 9(d), it can be seen that there were some particles that were not fully adhered to the surface of the carbon felt. This explains the deterioration in the electrochemical activity of the produced electrode. The aggregation of particles also reduces the electrochemical activity of the electrodes due to lessened active sites [43].

For the one deposited at -1.0 V potential, lesser deposition can be observed. Based on Figure 9(e), the surface of the carbon felt was flaky, indicating electrochemically aged felt [44]. There were irregular and larger aggregates on the surface. Similarly, these can be observed in felt deposited at -1.2 V too. This is due to the damage caused by the hydrogen evolution reaction that occurred during the deposition at both potentials. The electrode showed agglomeration, with larger flakes and loosely attached clusters (Figure 9(f)). This indicates over-deposition and poor adhesion as a result of excessive metal reduction.

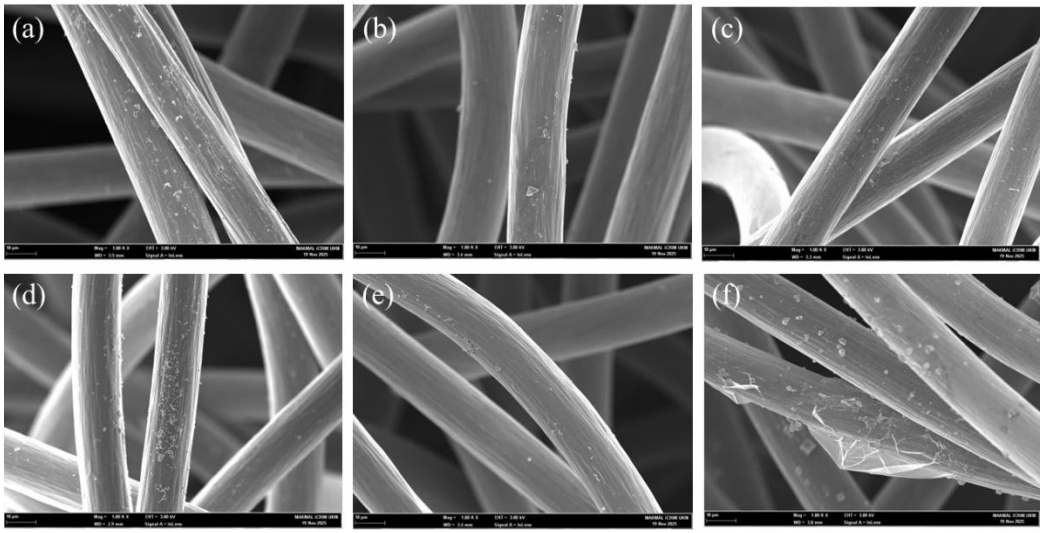

Figure 8. SEM micrographs of SnCo deposited carbon felts at (a) -0.2 V, (b) -0.4 V, (c) -0.6 V (d) -0.8 V (e) -1.0 V (f) -1.2 V captured at 1000× magnification

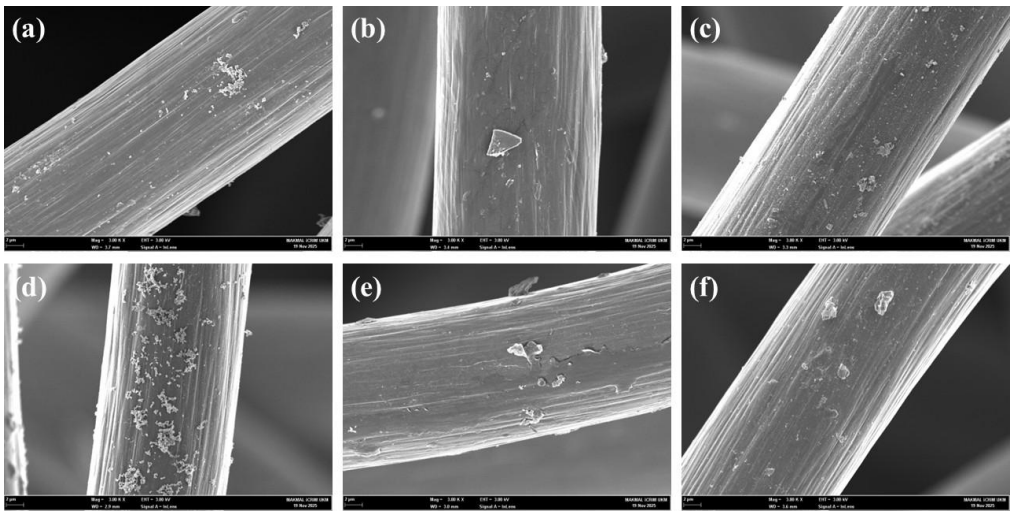

Figure 9. SEM micrographs of SnCo deposited carbon felts at (a) -0.2 V, (b) -0.4 V, (c) -0.6 V (d) -0.8 V (e) -1.0 V (f) -1.2 V captured at 3000× magnification

Figure 10 shows the SEM micrographs of SnCo deposited carbon cloths using different Sn:Co ratios. SnCo 1:1 electrode showed defined and uniform coating with smooth surface texture that adhered closely to the carbon cloth substrate. This proves that EDTA produces effective coordination with the metal ions enabling controlled co-deposition with the absence of large agglomerates and homogenous particle distribution. As the cobalt content increased to a SnCo ratio of 1:2, the electrode maintained similar uniformity as SnCo 1:1, with fewer larger grains and smoother surface. The higher cobalt concentration can increase surface area that may lead to enhanced capacitive behaviour.

At the highest ratio, the SnCo 1:4 electrode resulted the least favourable morphology, with very thin layer of catalyst coverage. Large areas of the underlying carbon cloth remained exposed, suggesting poor deposition efficiency likely caused by unfavourable deposition kinetics and ion imbalance. For the SnCo catalyst, the well-dispersed coated surfaces sample provide larger surface area and enhance adsorption of oxygen molecules onto the cathode. The high surface area of the catalyst is expected to substantially increase the oxygen reaction rate and electron acceptance, which is beneficial for boosting cathodic performance in MFCs. Previous research has highlighted the importance of nano-scale uniformity in enhancing electrocatalytic activity and aiding reactant diffusion within fuel cell system [45],[46]. The results obtained are consistent with these findings, demonstrating that precise control over synthesis parameters, particularly the metal ratio which can influence the catalyst's surface structure and its performance in electrochemical systems.

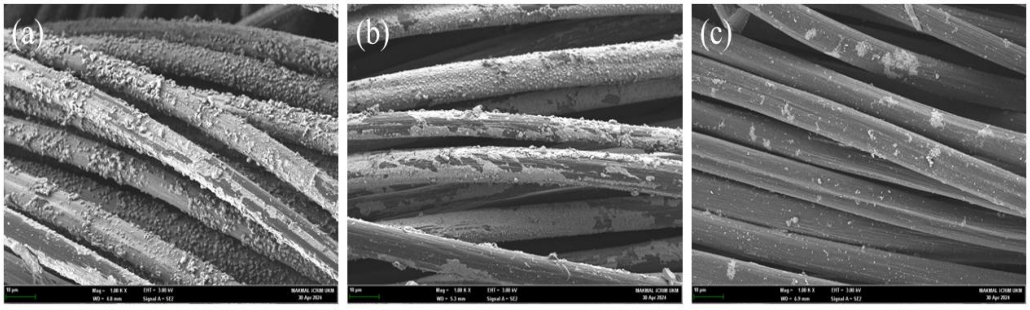

Figure 10. SEM micrographs of SnCo deposited carbon cloths with (a) 1:1 ratio, (b) 1:2 ratio and (c) 1:4 ratio

Comparison of SnCo deposited carbon felts and carbon cloths

For the surface analysis, the SEM micrographs with 1000× magnifications were compared. It can be seen that SnCo deposited on carbon cloths are more uniform compared to carbon felts. The adherence of deposits on carbon felts also less than carbon cloths. The differences are due to the different mode of deposition. Carbon cloths were deposited using CV whereas carbon felts were deposited using chronoamperometry using single and consistent potential throughout the deposition. CV used wide range of potential. This wide range of potential might have given more uniform deposits due to different and changing rate of nucleation throughout the deposition. The nature of structure of carbon felts and carbon cloths also affected the deposition distribution [47].

For the CV analysis of SnCo deposited carbon felts in saturated-CO_2, it was deduced that the CO_2 reduction indeed occurred for all electrodes compared to control undeposited carbon felts. This shows that SnCo deposited carbon felts do have the potential in the application of reducing CO_2 from wastewater. The one deposited at -0.6 V potential recorded the highest current density. Although the CO_2RR analysis provides useful information on the cathodic reduction behaviour of SnCo-deposited carbon felt, the findings are interpreted within the scope of electrochemical screening. The CO_2RR analysis in phosphate buffer at pH 7 was conducted as a controlled electrochemical screening test to evaluate the cathodic reduction behaviour of SnCo-deposited carbon felt under neutral aqueous conditions. However, this condition does not fully represent the complete operating environment of an MFC cathode. Therefore, the CO_2RR result should be interpreted as a supporting electrochemical evaluation of SnCo catalytic behaviour for cathodic reduction. In this study, the MFC performance evaluation was conducted only using SnCo-deposited carbon cloth, where the catalyst was assessed through O_2RR activity, stability and reactor-level power generation. Further studies under actual MFC cathode conditions are required to confirm the role of SnCo-deposited carbon felt for practical CO_2 reduction applications.

For SnCo deposited carbon cloths, the CV showed that all the electrodes with different ratios showed good O_2RR activity. This proved their efficiency in completing MFC circuit as well as aiding the energy generation. Due to SnCo deposited carbon cloth having high current retention and stability in O_2-saturated condition, the SnCo deposited cloth were applied in MFC. SnCo deposited carbon cloth also showed good O_2RR activity which was necessary to complete the circuit in MFC. While the efficiency of CO_2 reduction has been proven for the carbon felts, however, the stability of the produced electrodes can still be enhanced. Therefore, the carbon cloth-based O_2RR and MFC results were used as the direct evaluation of SnCo cathode performance in the present study.

Response surface methodology

Table 2 shows the statistics of quadratic regression model. A quadratic response surface regression model was fitted to evaluate the combined influence of electrodeposition potential and Co compositional ratio on the electrochemical response. The model exhibits good predictive capability, with a coefficient of determination $R^2 = 0.78$ and an adjusted $R^2 = 0.75$.

Table 2. Quadratic regression model statistics.

Regression Statistics	
Multiple R	0.88
R Square	0.78
Adjusted R Square	0.75
Standard Error	0.14
Observations	48

Table 3 and 4 show the results the quadratic regression model in the form of analysis of variance (ANOVA). ANOVA confirms that the overall model is highly statistically significant with F = 29.64 and Prob.> F = 9.28×10^{-13} which indicates that the selected parameters collectively exert a strong influence on the response.

The results of individual regression terms reveal that deposition potential is the dominant factor that influences the behaviour of the system. Both the linear potential term ($p = 1.70 \times 10^{-12}$) and the quadratic potential term ($p = 2.08 \times 10^{-14}$) are highly significant, confirming the presence of distinct curvature and

an interior optimum in the response surface. In contrast, the Co compositional ratio exhibits a weaker linear contribution. As shown in Table 4, the quadratic and interaction terms are not statistically significant, suggesting a monotonic compositional effect without strong curvature or synergistic interaction within the studied range.

Table 3. Quadratic regression model in ANOVA.

	DF	Sum of square	Mean Square	F	Prob. > F
Model	5	3.07	0.61	29.64	9.28×10^{-13}
Residual	42	0.87	0.02		
Total	47	3.94	0.63		

Table 4. ANOVA of individual regression terms.

	Coefficients	Standard Error	t Stat	p-value	
Intercept	-0.94	0.19	-4.83	1.83×10^{-05}	
Co	0.18	0.12	1.47	0.15	Non-significant
Potential_V	-3.47	0.35	-9.86	1.70×10^{-12}	Highly significant
Co_sq	-0.02	0.02	-0.82	0.41	Non-significant
V_sq	-2.45	0.22	-11.38	2.08×10^{-14}	Highly significant
Co_V	-0.002	0.07	-0.03	0.97	Non-significant

A three-dimensional response surface was constructed to describe the combined influence of deposition potential, applied during SnCo electrodeposition on carbon felt, and the Sn:Co compositional ratio employed for carbon cloth on the overall catalytic performance (Figure 11). The two substrates contribute to different electrochemical pathways which are CO_2 reduction on the felt and O_2 reduction on the cloth. Hence, their responses were combined using a geometric desirability function (D), where D = 1 represents optimal co-performance and D = 0 represents the least favorable condition [48]. For the desirability analysis, the CO_2RR and O_2RR responses were first normalised into individual desirability values between 0 and 1, where 0 represents the least favourable response and 1 represents the most favourable response. The overall desirability value was calculated as $D = (d_{CO_2RR} \times d_{O_2RR})^{0.5}$, where dCO_2RR represents the desirability value for CO_2RR and dO_2RR represents the desirability value for O_2RR. Equal weighting was assigned to both responses because CO_2RR and O_2RR were treated as cathodic electrochemical screening indicators in this study. The normal probability plot of residuals obtained from the quadratic response surface model shows that the residuals follow an approximately linear trend, indicating that they are close to normally distributed (Figure S1). Minor deviations at the tails are observed and are attributed to experimental boundary conditions at low and high response values. The residuals are plotted against fitted values (Figure S2). The residuals are randomly scattered around the zero-reference line without systematic trends. This confirms the adequacy of the fitted quadratic model.

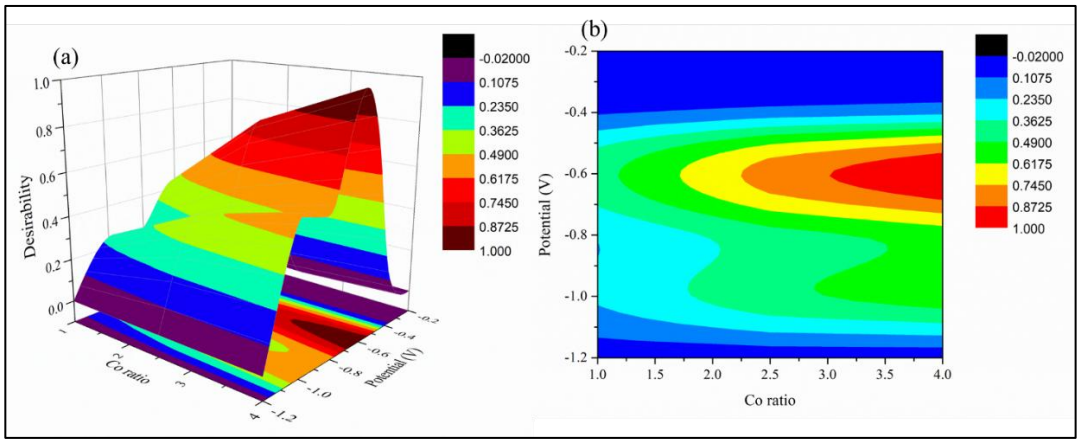

Figure 11. (a) 3D and (b) 2D response surface graphs of interaction of deposition potential and Co ratio based on CO_2RR and O_2RR

The resulting response surface exhibits a well-defined asymmetric maximum centered at a deposition potential of approximately -0.6 V and a Sn:Co ratio of 1:4. A curvature along the potential dimension can be observed, indicating a strong quadratic dependence of CO_2 reduction activity on electrodeposition potential. Near -0.6 V, the nucleation and growth of the Sn-rich catalytic phase are optimised, corresponding to the highest experimentally observed CO_2 reduction current density (1.09 mA cm^{-2}). Deviation toward either more positive or more negative potentials leads to deteriorating performance. For -0.2 V to -0.4 V, insufficient metallic Sn formation limits CO_2 activity, whereas for -0.8 V to -1.2 V, the low activity of CO_2 is caused by the change on morphology of electrodes. The changing of electrodes was caused by the competing hydrogen evolution during deposition [49]. This change suppresses adsorbed CO_2 intermediates, resulting in a sharp decline in desirability.

In contrast, along the Co composition axis, the response surface displays a monotonic increment. This is consistent with the approximately linear dependence of O_2RR activity on the Sn:Co ratio. The highest O_2RR performance is observed for the 1:4 Sn:Co composition, in agreement with the measured cathodic current density (-0.40 A), suggesting that increased Co incorporation enhances the density or stability of oxygen-binding active sites. The addition of Co increased the stability during nucleation by controlling the grain growth and the metal crystallization, improving the electrochemical properties as the ratio increases [50]. There is a smooth gradient along the axis. This shows that the compositional effects are continuous and predictable, with no evident quadratic curvature within the investigated range.

The combined response surface indicates a favourable electrochemical screening region in which the selected CO_2RR and O_2RR responses are simultaneously enhanced. The highest desirability value (D = 1.00) was obtained at a deposition potential of -0.60 V and a Sn:Co ratio of 1:4, corresponding to the most favourable combined electrochemical response within the studied screening conditions. The stronger curvature along the potential axis compared to the gradual compositional slope indicates that deposition potential has a greater influence on overall response variability. Therefore, the RSM result should be interpreted as an electrochemical screening outcome rather than a direct predictor of MFC power output. This provides useful information for selecting electrodeposition parameters that can enhance CO_2RR and O_2RR screening responses.

Finally, the smooth and continuous nature of the response surface, together with the absence of saddle points or discontinuities, supports the internal consistency of the experimental data. This also confirms the adequacy of the quadratic-linear RSM framework. The 3D model thus provides a strong graphical and quantitative description of how electrochemical and compositional parameters interact.

Microbial fuel cell performance

The Nyquist plots (Figure 12(a)) show all the SnCo modified cathodes resulting in lower internal resistance (Rint) compared to the control. Among them, the SnCo 1:1 exhibited low charge transfer resistance (3.57 Ω), followed closely by SnCo 1:2 (3.88 Ω), indicating more efficient electron transport across the electrode–electrolyte interface. The reduced semicircle diameters observed for these two electrodes reflect enhanced electrochemical kinetics, likely due to better catalyst dispersion and enhanced active site accessibility, as confirmed by morphological analysis. Furthermore, the SnCo 1:2 cathode achieved the highest maximum power density (0.105 W/m^2), followed by SnCo 1:1 (0.089

W/m^2), SnCo 1:4 (0.069 W/m2) as presented in Figure 12(b). This trend correlates well with the impedance results, reinforcing the role of optimized Sn:Co ratios and chelating agent selection in enhancing catalytic efficiency.

In the polarization curves (Figure 12(c)), the SnCo 1:1 & 1:2 electrode also demonstrated slower voltage drop with increasing current density, indicating better electrocatalytic stability and improved overall cell performance. This enhanced behavior can be attributed to a combination of optimized metal interaction, uniform surface morphology, and balanced conductivity between Co (as the O_2RR-active site) and Sn (as a stabilizing agent). These performances do align with past studies that had previously reported maximum output efficiency in MFCs using balanced bimetallic or composite catalysts [51]. Taken together, the findings affirm that the SnCo 1:1 & 1:2 composition offers good electrochemical and power generation characteristics suitable for sustainable energy applications.

Although SnCo 1:4 showed favourable electrochemical response in the RSM screening, its performance in the MFC system was lower than SnCo 1:1 and SnCo 1:2. This difference indicates that the electrochemical screening result and whole-cell MFC performance are influenced by different factors. The RSM result was based on selected CO_2RR and O_2RR responses under controlled electrochemical conditions, whereas the MFC performance was affected by reactor-level factors such as microbial electron transfer, oxygen supply, circuit resistance, proton transfer, pH, concentration and cathodic reduction behaviour [12]. Therefore, SnCo 1:2 showed better practical MFC performance because it provided a more balanced catalytic activity, stability and charge transfer behaviour compared to SnCo 1:4.

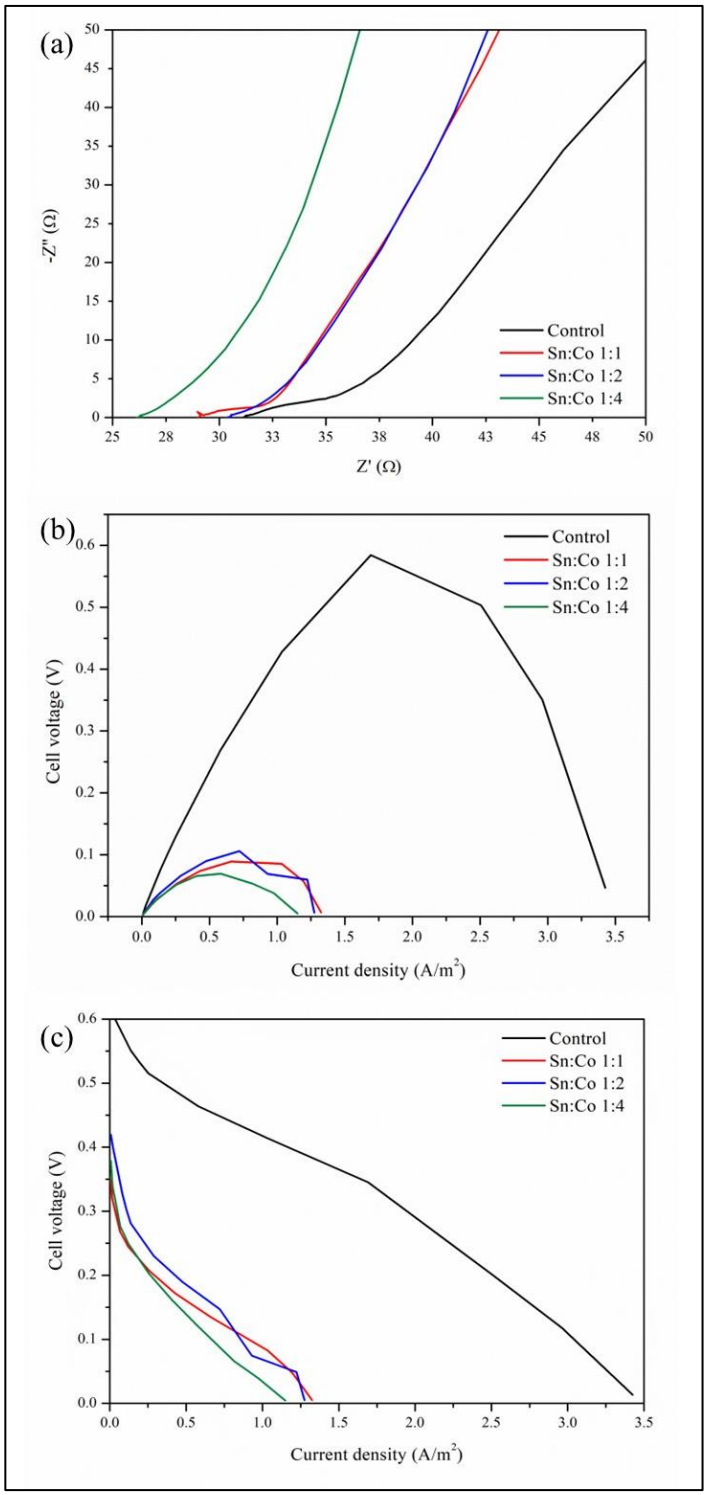

Figure 12. (a) Nyquist plots, (b) power density curves and (c) polarisation curves of MFCs at different ratios of SnCo

The observed enhancement in performance for the SnCo 1:1 & 1:2 catalyst can be explained by a combination of structural, electronic, and compositional factors. Sn contributes to surface stabilization and enhanced electron mobility, while Co provides efficient O_2RR-active sites [46], [52], [53]. The synergistic interaction between these metals likely enhances the binding of oxygen intermediates and facilitates their reduction, resulting in improved catalytic efficiency. The optimized morphology, including

increased porosity and homogeneous particle distribution, further supports effective mass transport and reduces charge transfer resistance, making the catalyst suitable for real-world MFC operations. From a practical perspective, the use of abundant, low-cost materials such as Sn and Co provides a sustainable alternative to conventional noble metal catalysts like platinum, Pt which are expensive and susceptible to poisoning [54]. These results highlight the importance of rational material design, specifically in tailoring metal ratios and synthesis conditions, to develop next generation electrocatalysts for wastewater treatment and renewable energy applications.

Conclusions

In conclusion, SnCo bifunctional electrocatalysts with varying deposition potentials and Sn:Co ratios were investigated as cost-effective alternatives to platinum-based cathodes in microbial fuel cell applications. The study of the potentials was done on carbon felts whereas the study of ratios was done on carbon cloths. Based on the findings, SnCo deposited carbon felts showed good CO_2RR activity. The carbon felt deposited at the potential -0.6 V exhibited the best CO_2RR performance. The CO_2RR performance proved the potential of carbon felts deposited electrodes as cathodes in the future applications, especially MFC. Optimisation using RSM also indicated the potential used for carbon felts deposition is the dominant parameters affecting the performance. This strongly justifies further targeted investigation of carbon felts for MFC applications. For carbon cloths, SnCo 1:1 & 1:2 catalyst demonstrated the most favourable electrochemical and morphological characteristics, leading to enhanced O_2RR activity, reduced internal resistance, and the highest power output among all tested modified electrodes. All the SnCo modified carbon cloth electrodes exhibited improved oxygen reduction performance in neutral conditions, the catalysts showing high current retention and charge transfer capability compared to unmodified carbon cloth. Due to the low cost and high availability of Sn and Co precursors, the developed SnCo catalysts present a promising alternative to platinum, offering both economic and operational advantages for large-scale, sustainable MFC applications.

Conflicts of Interest

The authors declare that there is no conflict of interest regarding the publication of this paper.

Acknowledgment

The authors would like to thank Universiti Kebangsaan Malaysia for the financial support provided through the Geran Translasi (UKM-TR2024-20) and Ministry of Higher Education (MoHE), Malaysia, through the Higher Education Centre of Excellence (HiCoE) SELFUEL research grant (HICOE-2023-003). The authors gratefully acknowledge Mohd Asri Yusof, Mohd Fareeq Ahmad Fudzi, and Nik Samila Che Yusoff for their invaluable assistance with the electrical setup, sensor fabrication, and laboratory operations.

References

[1] L. J. R. Nunes, “The Rising Threat of Atmospheric CO2: A Review on the Causes, Impacts, and Mitigation Strategies,” *Environments - MDPI*, 10(4), 2023. https://doi.org/10.3390/environments10040066

[2] R. M. Venegas, J. Acevedo, and E. A. Treml, “Three decades of ocean warming impacts on marine ecosystems: A review and perspective,” *Deep Sea Res 2 Top Stud Oceanogr*, 212, p. 105318, 2023. https://doi.org/10.1016/j.dsr2.2023.105318

[3] V. Davtyan, “International Energy Agency,” *Elgar Encyclopedia of Energy Economics*, pp. 294–296, 2025. https://doi.org/10.4337/9781035310371.00082

[4] X. P. Nguyen, A. T. Hoang, A. I. Ölçer, and T. T. Huynh, “Record decline in global CO2 emissions prompted by COVID-19 pandemic and its implications on future climate change policies,” *Energy Sources, Part A: Recovery, Utilization and Environmental Effects*, vol. 47(1), pp. 4699–4702, 2025. https://doi.org/10.1080/15567036.2021.1879969

[5] S. Norasyiqin *et al.*, “The Trend and Status of Energy Resources and Greenhouse Gas Emissions in the Malaysia Power Generation Mix,” *Energies (Basel)*, vol. 14, no. 2200, pp. 1–26, 2021.

[6] E. Ranieri *et al.*, “Evaluation of greenhouse gas emissions from aerobic and anaerobic wastewater treatment plants in Southeast of Italy,” *J Environ Manage*, vol. 337, no. March, p. 117767, 2023. https://doi.org/10.1016/j.jenvman.2023.117767

[7] R. Boiocchi *et al.*, “A study on the carbon footprint contributions from a large wastewater treatment plant,” *Energy Reports*, vol. 9, no. February, pp. 274–286, 2023. https://doi.org/10.1016/j.egyr.2023.06.002

[8] Y. Wu *et al.*, “Achieving high power density and excellent durability for high temperature proton exchange membrane fuel cells based on crosslinked branched polybenzimidazole and metal-organic frameworks,” *J Memb Sci*, vol. 630, no. January, p. 119288, 2021. https://doi.org/10.1016/j.memsci.2021.119288

[9] T. C. Dakal *et al.*, "New horizons in microbial fuel cell technology: applications, challenges, and prospects," *Biotechnology for Biofuels and Bioproducts*, 18(1) 2025. https://doi.org/10.1186/s13068-025-02649-y

[10] D. Ucar, Y. Zhang, and I. Angelidaki, "An overview of electron acceptors in microbial fuel cells," *Front Microbiol*, vol. 8, no. APR, pp. 1–14, 2017. https://doi.org/10.3389/fmicb.2017.00643
R. Boukoureshtlieva, T. Stankulov, and A. Momchilov, "Carbon-Based Cathode Catalysts Used in Microbial Fuel Cells for Wastewater Treatment and Energy Recovery," Ecological Engineering and Environment Protection, vol. 2021, no. 3/2021, pp. 24–33, 2021. https://doi.org/10.32006/eeep.2021.3.2433

[11] K. Elangovan et al., "Outline of microbial fuel cells technology and their significant developments, challenges, and prospects of oxygen reduction electrocatalysts," Frontiers in Chemical Engineering, 5, pp. 1–27, 2023. https://doi.org/10.3389/fceng.2023.1228510

[12] R. Agrahari, B. Bayar, H. N. Abubackar, B. S. Giri, E. R. Rene, and R. Rani, "Advances in the development of electrode materials for improving the reactor kinetics in microbial fuel cells," Chemosphere, 290, 2022. https://doi.org/10.1016/j.chemosphere.2021.133184

[13] A. Chaturvedi and P. P. Kundu, "Recent advances and perspectives in platinum-free cathode catalysts in microbial fuel cells," J Environ Chem Eng, 9(4), p. 105662, 2021. https://doi.org/10.1016/j.jece.2021.105662

[14] N. Helsel and P. Choudhury, "Non-Platinum Group Metal Oxygen Reduction Catalysts for a Hydrogen Fuel Cell Cathode: A Mini-Review," Catalysts, 15(6), 2025. https://doi.org/10.3390/catal15060588

[15] S. Karthick, A. Sumisha, and K. H. Haribabu, "Performance of tungsten oxide/polypyrrole composite as cathode catalyst in single chamber microbial fuel cell," J Environ Chem Eng, 8(6), p. 104520, 2020. https://doi.org/10.1016/j.jece.2020.104520

[16] F. Lan, G. Huang, Y. Cao, X. Zhang, R. Wang, and J. Chen, "Enhancing oxygen reduction reaction in microbial fuel cell by Cu-metal organic framework@Fe-metal organic framework (Cu-MOF@Fe-MOF) as cathode catalyst," J Environ Chem Eng, 13(2), p. 115448, 2025. https://doi.org/10.1016/j.jece.2025.115448

[17] M. Li, J. Zhou, Y. G. Bi, S. Q. Zhou, and C. H. Mo, "Transition metals (Co, Mn, Cu) based composites as catalyst in microbial fuel cells application: The effect of catalyst composition," *Chemical Engineering Journal*, 383, p. 123152, 2020. https://doi.org/10.1016/j.cej.2019.123152

[18] S. Ashmath, H. J. Kwon, S. G. Peera, and T. G. Lee, "Solid-State Synthesis of Cobalt/NCS Electrocatalyst for Oxygen Reduction Reaction in Dual Chamber Microbial Fuel Cells," *Nanomaterials*, 12(24), 2022. https://doi.org/10.3390/nano12244369

[19] W. Liu, L. Zheng, S. Cheng, Y. Zhu, and J. Sun, "Cobalt nitrogen carbon nanotube co-implanted activated carbon as efficient cathodic oxygen reduction catalyst in microbial fuel cells," *Journal of Electroanalytical Chemistry*, 876, 2020. https://doi.org/10.1016/j.jelechem.2020.114498

[20] M. Li et al., "Cobalt-based Catalysts Modified Cathode for Enhancing Bioelectricity Generation and Wastewater Treatment in Air-breathing Cathode Microbial Fuel Cells," Electroanalysis, 31(8), pp. 1482–1493, 2019. https://doi.org/10.1002/elan.201900161

[21] X. M. Qu et al., "In-situ growth of carbon nanotubes for improving the performance of Co-N/C catalysts in proton exchange membrane fuel cell," Chemical Engineering Journal, vol. 461, no. February, 2023. https://doi.org/10.1016/j.cej.2023.142054

[22] S. Zhao et al., "Advances in Sn-Based Catalysts for Electrochemical CO2 Reduction," Nanomicro Lett, 11(1), pp. 1–19, 2019. https://doi.org/10.1007/s40820-019-0293-x

[23] X. Tu, X. Liu, Y. Zhang, J. Zhu, and H. Jiang, "Advances in Sn-based oxide catalysts for the electroreduction of CO2 to formate," Green Carbon, 2(2), pp. 131–148, 2024. https://doi.org/10.1016/j.greenca.2024.03.006

[24] R. K. Dharman, A. Mariappan, H. M. Lo, and T. H. Oh, "Kinetically accelerated bifunctional water splitting performance using tin-induced cobalt molybdate electrocatalyst," Inorg Chem Commun, 183 (P1), p. 115725, 2026. https://doi.org/10.1016/j.inoche.2025.115725

[25] S. S. Lim, J. M. Fontmorin, M. N. Ikhmal Salehmin, Y. Feng, K. Scott, and E. H. Yu, "Enhancing hydrogen production through anode fed-batch mode and controlled cell voltage in a microbial electrolysis cell fully catalysed by microorganisms," Chemosphere, 288(P2), p. 132548, 2022. https://doi.org/10.1016/j.chemosphere.2021.132548

[26] G. Pignol, P. Bassil, J. M. Fontmorin, D. Floner, F. Geneste, and P. Hapiot, "Electrochemical Properties of Carbon Fibers from Felts" Molecules, 27(19), 2022. https://doi.org/10.3390/molecules27196584

[27] D. Emmel, J. D. Hofmann, T. Arlt, I. Manke, G. D. Wehinger, and D. Schröder, "Understanding the Impact of Compression on the Active Area of Carbon Felt Electrodes for Redox Flow Batteries," ACS Appl Energy Mater, 3(5), pp. 4384–4393, 2020. https://doi.org/10.1021/acsaem.0c00075

[28] Y. Du, R. Kang, B. Zhang, H. Wang, G. Chen, and J. Zhang, "Retarding Deposition and Hydrogen Evolution Reaction Enables Stable and Reversible Zn Metal Anode," ACS Energy Lett, 9(3), pp. 967–975, 2024. https://doi.org/10.1021/acsenergylett.4c00347

[29] J. Huang et al., "Effect of deposition potential on electrodeposition of Sn-Ag-Cu ternary alloy solderable coating in deep eutectic solvent," *Journal of Electroanalytical Chemistry*, 943, no. April, p. 117613, 2023. https://doi.org/10.1016/j.jelechem.2023.117613

[30] A. Boukhouiete, S. Boumendjel, and N. E. H. Sobhi, "Effect of current density on the microstructure and morphology of the electrodeposited nickel coatings," *Turk J Chem*, 45(5), pp. 1599–1608, 2021. https://doi.org/10.3906/kim-2102-46

[31] S. Saini, S. C. Wright, S. Parvin, J. Baltrusaitis, and M. T. McDowell, "Investigating the Effects of Copper Impurity Deposition on the Structure and Electrochemical Behavior of Hydrogen Evolution Electrocatalyst Materials," *ACS Appl Energy Mater*, 8(2), pp. 1143–1153, 2025. https://doi.org/10.1021/acsaem.4c02697

[32] A. Raveendran, M. Chandran, and R. Dhanusuraman, "A comprehensive review on the electrochemical parameters and recent material development of electrochemical water splitting electrocatalysts," *RSC Adv*, 13(6), pp. 3843–3876, 2023.

https://doi.org/10.1039/d2ra07642j

[33] W. Yu, H. Jiang, and Z. Hou, "Nanocurved electric-field-induced optimal catalyst loading for carbon dioxide electroreduction," *Phys Rev Res*, 5(4) 2023. https://doi.org/10.1103/PhysRevResearch.5.043235

[34] M. Tribbia, J. Glenneberg, F. La Mantia, and G. Zampardi, "Effect of the Current Density on the Electrodeposition Efficiency of Zinc in Aqueous Zinc-Ion Batteries," *ChemElectroChem*, 11(1), 2024. https://doi.org/10.1002/celc.202300394

[35] D. Kong et al., "Inhibition of hydrogen evolution reaction during iron electrodeposition from sulfate system by reducing hydrogen bonding activity in water," *Int J Hydrogen Energy*, 191, p. 152286, 2025. https://doi.org/10.1016/j.ijhydene.2025.152286

[36] E. P. Barbano, G. M. de Oliveira, M. F. de Carvalho, and I. A. Carlos, "Copper-tin electrodeposition from an acid solution containing EDTA added," *Surf Coat Technol*, 240, pp. 14–22, 2014. https://doi.org/10.1016/j.surfcoat.2013.12.005

F. Luo et al., "P-block single-metal-site tin/nitrogen-doped carbon fuel cell cathode catalyst for oxygen reduction reaction," *Nat Mater*, 19(11), pp. 1215–1223, 2020. https://doi.org/10.1038/s41563-020-0717-5

[37] K. Ye et al., "Synergy effects on Sn-Cu alloy catalyst for efficient CO2 electroreduction to formate with high mass activity," *Sci Bull (Beijing)*, 65(9), pp. 711–719, 2020. https://doi.org/10.1016/j.scib.2020.01.020

[38] B. G. Abraham, R. Bhaskaran, and R. Chetty, "Electrodeposited Bimetallic (PtPd, PtRu, PtSn) Catalysts on Titanium Support for Methanol Oxidation in Direct Methanol Fuel Cells," J Electrochem Soc, 167(2), p. 024512, 2020. https://doi.org/10.1149/1945-7111/ab6a7d

S. Jiang, L. Zhu, Z. Yang, and Y. Wang, "Self-supported hierarchical porous FeNiCo-based amorphous alloys as high-efficiency bifunctional electrocatalysts toward overall water splitting," Int J Hydrogen Energy, 46(74), pp. 36731–36741, 2021. https://doi.org/10.1016/j.ijhydene.2021.08.223

[39] M. Wang et al., "Colloids and Surfaces A : Physicochemical and Engineering Aspects Enhancing electrochemical CO 2 reduction by utilizing tin-based gas diffusion electrodes with cubic nanostructured Cu 2 O as an interlayer carrier," Colloids Surf A Physicochem Eng Asp, 726(P1), p. 137740, 2025. https://doi.org/10.1016/j.colsurfa.2025.137740

[40] S. Li et al., "International Journal of Hydrogen Energy Recent advances in the development of single atom catalysts for oxygen evolution reaction, 82, pp. 1081–1100, 2024. https://doi.org/10.1016/j.ijhydene.2024.08.026

[41] L. Eifert, R. Banerjee, Z. Jusys, and R. Zeis, "Characterization of Carbon Felt Electrodes for Vanadium Redox Flow Batteries: Impact of Treatment Methods," J Electrochem Soc, 165(11), pp. A2577–A2586, 2018. https://doi.org/10.1149/2.0531811jes

[42] Y. Chen, Huina, Jian, Demin, Xie, Hao, Liu, Yuxin, Li, Shishi, Wang, "Cu2O@Co/N-doped carbon as antibacterial catalysts for oxygen reduction in microbial fuel cells," Environ Sci Nano, 10(1), pp. 158–165, 2023. https://doi.org/10.1039/D2EN00980C

[43] Y. Sun, H. Li, S. Guo, and C. Li, "Metal-based cathode catalysts for electrocatalytic ORR in microbial fuel cells: A review," Chinese Chemical Letters, 35(5), p. 109418, 2024. https://doi.org/10.1016/j.cclet.2023.109418

[44] J. Tian et al., "Effects of the Intrinsic Structures of Graphite Felt and Carbon Cloth on the Working Condition of Iron-Chromium Redox Flow Batteries," 2025.

[45] R. Amdoun et al., "The Desirability Optimization Methodology; a Tool to Predict Two Antagonist Responses in Biotechnological Systems: Case of Biomass Growth and Hyoscyamine Content in Elicited Datura starmonium Hairy Roots," *Iran J Biotechnol*, 16(1), pp. 11–19, Feb. 2018. https://doi.org/10.21859/ijb.1339

[46] P. H. He, C. Y. Chiang, J. C. Yu, E. C. Liu, and C. N. Liao, "Effect of hydrogen evolution on morphology and capillary performance of electrodeposited copper wicks," *Mater Chem Phys*, 337, 2025. https://doi.org/10.1016/j.matchemphys.2025.130560

[47] F. Nacimiento, R. Alcántara, and J. L. Tirado, "Comparative study of composite electrodes containing tin, polyacrylonitrile and cobalt or iron," J Power Sources, 196(5), pp. 2893–2898, Mar. 2011. https://doi.org/10.1016/j.jpowsour.2010.11.034

[48] S. Singh, A.K., Gangwar, Agendra, Kumar, "Prospects and limitations of existing biofuels and emerging trends in the utilization of nanoparticles for enhanced biofuel production and microbial fuel cell efficiency," Biofuels, 16(5), 2025. https://doi.org/10.1080/17597269.2024.2431766

[49] R. Nurzulaikha et al., "Graphene/SnO2 nanocomposite-modified electrode for electrochemical detection of dopamine," Sens Biosensing Res, 5, pp. 42–49, 2015. https://doi.org/10.1016/j.sbsr.2015.06.002

[50] S. Gupta, R. Fernandes, R. Patel, M. Spreitzer, and N. Patel, "A review of cobalt-based catalysts for sustainable energy and environmental applications," Appl Catal A Gen, 661, 2023. https://doi.org/10.1016/j.apcata.2023.119254

[51] K. Ben, W. Ramli, W. Daud, and M. Ghasemi, "ScienceDirect Non-Pt catalyst as oxygen reduction reaction in microbial fuel cells: A review," Int J Hydrogen Energy, 39(10), pp. 4870–4883, 2014. https://doi.org/10.1016/j.ijhydene.2014.01.062